SLAS Discovery 35 (2025) 100259

Contents lists available at ScienceDirect

SLAS Discovery

journal homepage: www.elsevier.com/locate/slasd

Full Length Article

Aurora 2.0: A fluorogenic dye library for expanding the capability of protein-adaptive differential scanning fluorimetry (paDSF)

Annemarie F. Charvat [a,b,1], Kayleigh Mason-Chalmers [a,1], Aneta Grabinska-Rogala [a], Shloka Shivakumar [a], Zachary Gale-Day [a,b], Taiasean Wu [a,b], Zoe Millbern [c], Jonathan B. Grimm [d], Emma C. Carroll [a,b,e], K. Peter R. Nilsson [f], Luke D. Lavis [d], Nelson R. Vinueza [c], Jason E. Gestwicki [a,b,*]

[a] Institute for Neurodegenerative Diseases, University of California, San Francisco, San Francisco, CA 94158, USA
[b] Department of Pharmaceutical Chemistry, University of California San Francisco, San Francisco, CA 94158, USA
[c] Department of Textile Engineering, Chemistry and Science, North Carolina State University, Raleigh, NC 27695, USA
[d] Janelia Research Campus, Howard Hughes Medical Institute
[e] Department of Chemistry, San José State University, San Jose, CA 95112, USA
[f] Science for Life Laboratory, KTH—Royal Institute of Technology SE-171 21 Stockholm, Sweden

ARTICLE INFO

Keywords:
Thermal shift assay
Thermofluor
Protein stability
Binding assay
High throughput screening
Fluorescent probes
Fluorescent dye

ABSTRACT

Differential Scanning Fluorimetry (DSF) is a biophysical assay that is used to estimate protein stability *in vitro*. In a DSF experiment, the increased fluorescence of a solvatochromatic dye, such as Sypro Orange, is used to detect the unfolding of a protein during heating. However, Sypro Orange is only compatible with a minority of proteins (< 30 %), limiting the scope of this method. We recently reported that protein-adaptive DSF (paDSF) can partially solve this problem, wherein the protein is initially pre-screened against ~300 chemically diverse dyes, termed the Aurora collection. While this approach significantly improves the number of targets amenable to DSF, it still fails to produce protein-dye pairs for some proteins. Here, we report the expansion of the dye collection to Aurora 2.0, which includes a total of 517 structurally diverse molecules and multiple new chemotypes. To assess performance, these dyes were screened against a panel of ~100 proteins, which were selected, in part, to represent the most challenging targets (*e.g.* small size). From this effort, Aurora 2.0 achieved an impressive success rate of 94 %, including producing dyes for some targets that were not matched in the original collection. These findings support the idea that larger, more chemically diverse libraries improve the likelihood of detecting melting transitions across a wider range of proteins. We propose that Aurora 2.0 makes paDSF an increasingly powerful method for studying protein stability, ligand binding and other biophysical properties in high throughput.

1. Introduction

Differential Scanning Fluorimetry (DSF) is an assay used to estimate the stability of a purified protein by measuring its apparent melting temperature (T_{ma}) [1,2]. In a typical DSF experiment, a target protein is mixed with a "turn-on" fluorescence dye, typically either Sypro Orange or 8-anilinonaphthalene-1-sulfonic acid (ANS). As the mixture is heated, the protein unfolds, revealing hydrophobic regions that were previously buried in the native state and resulting in increased fluorescence intensity of the solvatochromatic dye (Fig. 1**a**). The protein's T_{ma} value is then determined by calculating the half maximal of the temperature *vs.* fluorescence plot [3–5]. In turn, the T_{ma} value is a broadly useful measure of relative protein stability, such that DSF has been used to measure ligand binding [3], determine inhibitor selectivity [6], study cofactor

Abbreviations: ANS, 8-anilinonaphthalene-1-sulfonic acid; CTD, C-terminal domain; DSF, Differential scanning fluorimetry; JDP, J-domain protein; OOB, Out-of-bag; paDSF, Protein-adaptive differential scanning fluorimetry; PCA, Principal component analysis; PCR, polymerase chain reaction; T_{ma}, apparent melting temperature; TPR, tetratricopeptide repeat; ZF, zinc finger.

* Corresponding author at: University of California San Francisco, Sandler Center, 675 Nelson Rising Lane, Room 311, San Francisco CA 94158, USA.
E-mail address: jason.gestwicki@ucsf.edu (J.E. Gestwicki).

[1] These authors contributed equally to the work.

https://doi.org/10.1016/j.slasd.2025.100259
Received 13 July 2025; Received in revised form 4 August 2025; Accepted 7 August 2025
Available online 8 August 2025

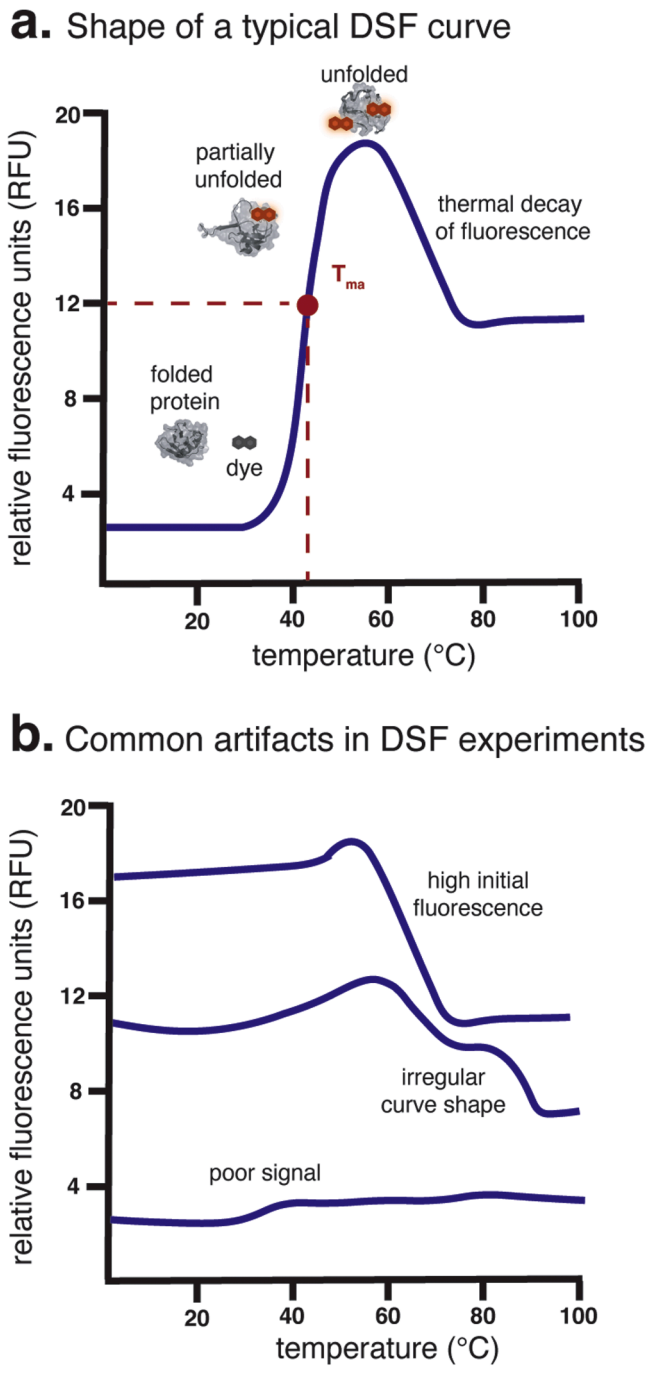

Fig. 1. Illustration of an idealized differential scanning fluorimetry (DSF) result and examples of common, obfuscating artifacts. (a) Example of an idealized DSF curve for a soluble, single-domain protein, in which dye fluorescence increases during thermal unfolding. Also, it is common for the signal to decay at higher temperatures, producing a characteristic curve shape. (b) Examples of common artifacts in DSF, such as high initial fluorescence, poorly defined transitions and/or no change in fluorescence upon protein unfolding. In all cases, it is not possible to calculate an accurate T_{ma} value.

interactions [7], optimize buffers [8–10] or additives [10] and study the impact of point mutations [11]. The shape of DSF curves has also been used to reveal the mechanism of inhibitors (*e.g.,* noncompetitive *vs*, covalent) [12]. Importantly, while other biophysical platforms can be used to acquire similar information, the advantage of DSF is that it can be carried out in high throughput [13,14]. For example, DSF has been used to perform large scale chemical screens in 384-well format [15,16], where a shift in the T_{ma} value (ΔT_{ma}) has been used to rapidly identify inhibitors. This method has also been used to profile large numbers of MHC-peptide interactions, with striking agreement to circular dichroism-based measurements of T_{ma} [17].

Despite the potential of DSF, several technical issues have limited its widespread use. One persistent problem is incompatibility of Sypro Orange with many proteins, plates, buffers and/or ligands [13]. These artifacts typically manifest as low dye fluorescence intensity, non-standard curve shapes and/or dye interactions with the folded state, all of which mask the unfolding transition (Fig. 1**b**) [18,19]. To address these issues, we recently introduced protein-adaptive Differential Scanning Fluorimetry (paDSF), an approach in which the assay is first "adapted" to the specific protein target (or application) by pre-screening it against a library of fluorogenic dyes to identify a compatible dye-protein pair [19]. Towards that goal, we collected a library of 312 dyes, termed Aurora, which includes a number of diverse chemotypes, including textile dyes, analogs of Sypro Orange and ANS, histology dyes, amyloid-binding ligands, laser dyes and a subset from the Max A. Weaver Collection [19,20]. When Aurora was screened against ~70 different test proteins, suitable paDSF dyes were identified for >90 %, strongly supporting the idea that failures in DSF are largely a product of incompatible dye reagents. A second important feature in the paDSF workflow is the use of DSFWorld software, which significantly improves the accuracy of T_{ma} determination by introducing new curve-fitting algorithms [4]. Together, these advancements in software and reagents expand the scope of paDSF experiments to allow studies of many more targets, including those with complex melting transitions. For example, paDSF was recently used to build an assay for the two-domain target, protein phosphatase 5 (PP5), which has complex unfolding behavior and was not compatible with Sypro Orange [21].

Despite these advances, some targets in the initial screening set were not matched to dyes in the Aurora collection. We hypothesize that a further expansion of the chemical, spectral and structural diversity of the dye library might further improve this platform. To test this idea, we created Aurora 2.0, an expanded collection comprising 517 total dyes. The new additions include scaffolds that were minimally explored in the original collection (now termed Aurora 1.0), such as rhodamines and polythiophenes. Screening Aurora 2.0 against 43 challenging proteins and a subset of the 70 original ones confirmed that it produced useful paDSF assays for 94 % of targets, including three that failed using Aurora 1.0 alone. In addition, we noticed that Aurora 2.0 included dyes that bind to the native, folded state, potentially providing "turn on" fluorescent probes for detecting these targets. We propose that Aurora 2.0 further expands the scope of paDSF, as well as providing dyes for additional applications.

2. Materials and methods

2.1. Aurora 2.0 collection

Sypro Orange (5000x) was purchased from Thermo Fischer Scientific (Ref S6650). The remaining dyes were obtained from collaborators [20, 22–26] or purchased from catalogs (**Supplementary Data 1**). Dyes were not further characterized. The Aurora 1.0 and extended library dyes were diluted to 1 mM (DMSO) and dispensed into clear 384-well microtiter plates (781,280, Greiner BioOne). These stock plates were sealed (Aluminum Nunc Sealing Tape C0T20240898) and stored at room temperature in the dark at room temperature (Aurora 1.0) or −20 °C (extended library).

For each member of the library, SMILES strings were canonicalized using Chem.MolToSmiles in the 'RDKit' package in Python 3. Molecular files were converted to 2048-bit Morgan Fingerprints and used to calculate a pairwise Tanimoto similarity matrix. The resulting similarity matrix was converted to a dissimilarity matrix by subtracting each value from 1. Butina clustering was performed in Python 3.0 to identify structurally similar scaffolds (**Supplementary Fig. 1a**), and a bar chart

was generated to compare differences (**Supplemental Fig. 1b**). Calculated LogP values were determined from the SMILES using Crippen. MolLogP from RDKit. To further analyze structural diversity, a Principal Component Analysis (PCA) was performed on the 2048-bit Morgan fingerprint matrix. This dimensionality reduction approach was implemented using the PCA class from sklearn.decomposition in the scikit-learn library, extracting the top two principal components. The components captured the axes of structural variation across the dye library.

2.2. Protein expression and purification

Proteins in the original test panel were described previously [19] and the 43 additional proteins were obtained from collaborators (see Acknowledgements). Each protein was stored and tested in its own buffer (**Supplemental Data 2**).

For the expression of DnaJ, DNAJA1, DNAJA2, DNAJB1, DNAJB2, DNAJB4, or DNAJC7, *Escherichia coli* Rosetta 2(DE3)pLysS cells were transformed with plasmids. The sequence of DnaJ was from *E. coli* and the remaining were human. Cells were grown in 2 L of Terrific Broth (TB) supplemented with either ampicillin (100 μg/ml) or kanamycin (50 μg/ml) at 37 °C. Protein expression was induced with 1 mM isopropyl β-d-thiogalactopyranoside (IPTG) at OD_{600} = 0.6, and cultures were incubated for 4 h at 37 °C. Cells were harvested by centrifugation, frozen, thawed, and lysed in buffer A (50 mM Tris–HCl pH 8.0, 300 mM NaCl, 10 % glycerol, 20 mM imidazole, 5 mM β-mercaptoethanol, 2 mM PMSF). Lysates were clarified by centrifugation (48,380 × *g*, 30 min, 4 °C), and the supernatants were loaded onto 5 mL of Ni-NTA resin (Thermo Scientific), pre-equilibrated with 20 mL of buffer A. The resin was washed sequentially with 40 mL of buffer A, 20 mL of buffer A containing 0.5 % Triton X-100, 20 ml of buffer A containing 700 mM NaCl, 20 mL of buffer A containing 0.1 mM ATP and 5 mM $MgCl_2$, and 20 mL of buffer A. Proteins were eluted with buffer A supplemented with 200 mM imidazole. Fractions containing the target JDPs were pooled and concentrated by centrifugation (3500 × *g*, 15 min, 4 °C) using Amicon® Ultra centrifugal filters with a 10 kDa molecular weight cut-off (Millipore). His-tags were removed by overnight incubation with TEV protease at 4 °C. Proteins were further purified by size-exclusion chromatography (SEC) on a HiLoad 16/600 Superdex 75 prep-grade column (Sigma-Aldrich) equilibrated in phosphate-buffered saline (PBS) supplemented with 1 mM DTT. Fractions with purified JDPs were pooled, concentrated using 10 kDa Amicon® Ultra filters (3500 × *g*, 15 min, 4 °C), aliquoted, flash-frozen in liquid nitrogen, and stored at −80 °C.

The DNAJB6b and DNAJB8 proteins were expressed in Rosetta 2 (DE3)pLysS cells harboring plasmids grown in 2 L TB medium supplemented with kanamycin (50 μg/mL) at 37 °C until reaching OD_{600} = 0.6. Protein expression was induced with 1 mM IPTG, and the cultures were incubated for an additional 3 h at 37 °C. Cells were harvested by centrifugation (4000 × *g*, 20 min, 4 °C), resuspended in PBS with 2.5 mM PMSF, and pelleted again. For lysis, cell pellets were resuspended in buffer E (8 M guanidine hydrochloride, 50 mM HEPES pH 7.5, 20 mM imidazole, 1 mM DTT). Lysates were clarified by centrifugation (10,000 × *g*, 20 min, 4 °C). The supernatant was loaded onto 5 mL of pre-equilibrated Ni-NTA resin (Thermo Scientific) with buffer E. The resin was washed sequentially with 50 mL of buffer E; 50 mL of buffer E without guanidine hydrochloride. Bound protein was eluted with 30 mL of elution buffer E with 500 mM imidazole. Fractions containing the target protein were dialyzed overnight at 4 °C in 5 L of 50 mM ammonium formate. Following lyophilization, protein samples were stored at −80 °C. In the psDSF experiments, these proteins were reconstituted in PBS containing 1 mM DTT.

2.3. Protein property analysis

Protein parameters, such as molecular weight, instability index, aliphatic index, GRAVY and residue information, were obtained by inputting protein sequence into Expasy ProtParam (see **Supplemental Data 2**). Protein models and tertiary structure information were obtained by inputting protein sequence into Alpha Fold 3.0. Percent disorder was calculated by taking the average residue disorder as found using MetaPredict V3.0 created by Alex Holehouse at Washington University. SASA was calculated using FreeSASA with the Shrake-Rupley algorithm [27].

2.4. Dye screening

Dye screens were performed as previously described [19] and a more detailed, step-by-step protocol has been reported [13]. From the stock dye plates, samples were dispensed into daughter plates (781,280, Greiner BioOne) and stored −20 °C. The daughter plate included 250 nL of each dye in DMSO and 20 μL of the desired buffer for each protein. The dye plate format for this dispensing step was adapted from previous reports [19]. Then, proteins (2 μL of 10 μM stock), were added to a 384-well, white, opaque Axygen (PCR-384-LC480WNF) microtiter plate. We find that white plates tend to have improved sensitivity in this application, while black qPCR plates tend to have reduced background. Therefore, we routinely use white plates for dye screens because signal intensity tends to be a more important experimental parameter in choosing dye-protein pairs than background signal, but this choice will sometimes depend on the specific application. To the Axygen plate was dispensed 8 μL of dye solution using an Opentrons OT-2. The plates were briefly spun before and after transfer of the dye solution. These plates were sealed (AB1 MicroAmp Optical Adhesive Film 4311,971) and DSF experiments performed in a qTOWER (Analytik Jena).

In each DSF experiment, fluorescence intensity was measured in six channels ('FAM' ex/em, 470/520; 'JOE' ex/em, 515 nm/545 nm; 'TAMRA' ex/em, 535 nm/580 nm; 'ROX' ex/em, 565 nm/605 nm; 'Cy5' ex/em, 630 nm/670 nm; 'Cy5.5' ex/em, 660 nm/705 nm). Each experiment was performed using a temperature range of 25 to 94 °C with a heating rate of 1 °C / min. If an individual protein did not unfold properly using this protocol, we tried "up-down" mode, as previously described [13]. Each experiment included an important control, in which buffer was used instead of protein. The data from the dye screens were analyzed using a previously described online tool [19]. Then, the T_{ma} values were calculated using DSFWorld [4]. From the curves with calculated values, "hits" were called manually if there was a clear sigmoidal increase in fluorescence in at least one of the ex/em channels. The "sensitives" were categorized as the samples in which the curve shape was not ideal, but there was an apparent increase in fluorescence. All other combinations were labelled as "inactive". Both the "hits" and "sensitives" were nominated for subsequent validation.

For validation, the "hits" and "sensitives" were carried forward to dose response experiments, as previously described [19]. Briefly, DSF experiments were repeated by varying the dye concentrations from 50 μM to 6.25 μM (2-fold dilutions), followed by screening using the same protocol as above (see **Supplemental Data 3**). The "hits" were then called manually if there was a clear sigmoidal increase in fluorescence that was dependent on the dye concentration. The T_{ma} values for the "hits" were calculated using DSFWorld [4].

2.5. Clustering of JDP similarity

To group the proteins, their J-domains were analyzed via the Smith-Waterman and Needleman-Wensch algorithms, which resulted in a dendrogram that aligned with their known phylogenetic relationships. This analysis also successfully clustered the proteins based on their known "A", "B" and "C" categories (*e.g.,* DnaJB1 and DnaJB4 clustered).

2.6. Statistics

A Pearson's Correlations Test was conducted to analyze the T_{ma} values and to explore potential trends between the percent disorder and number of "hit" dyes. A Fishers Exact Test was used to determine the

usefulness of each dye library, and a Wilcoxon's rank-sum test used to analyze their hit distributions. A Random Forest Classifier was used to predict whether a dye was active using its PCA values. All analyses were conducted using R v4.5.0.

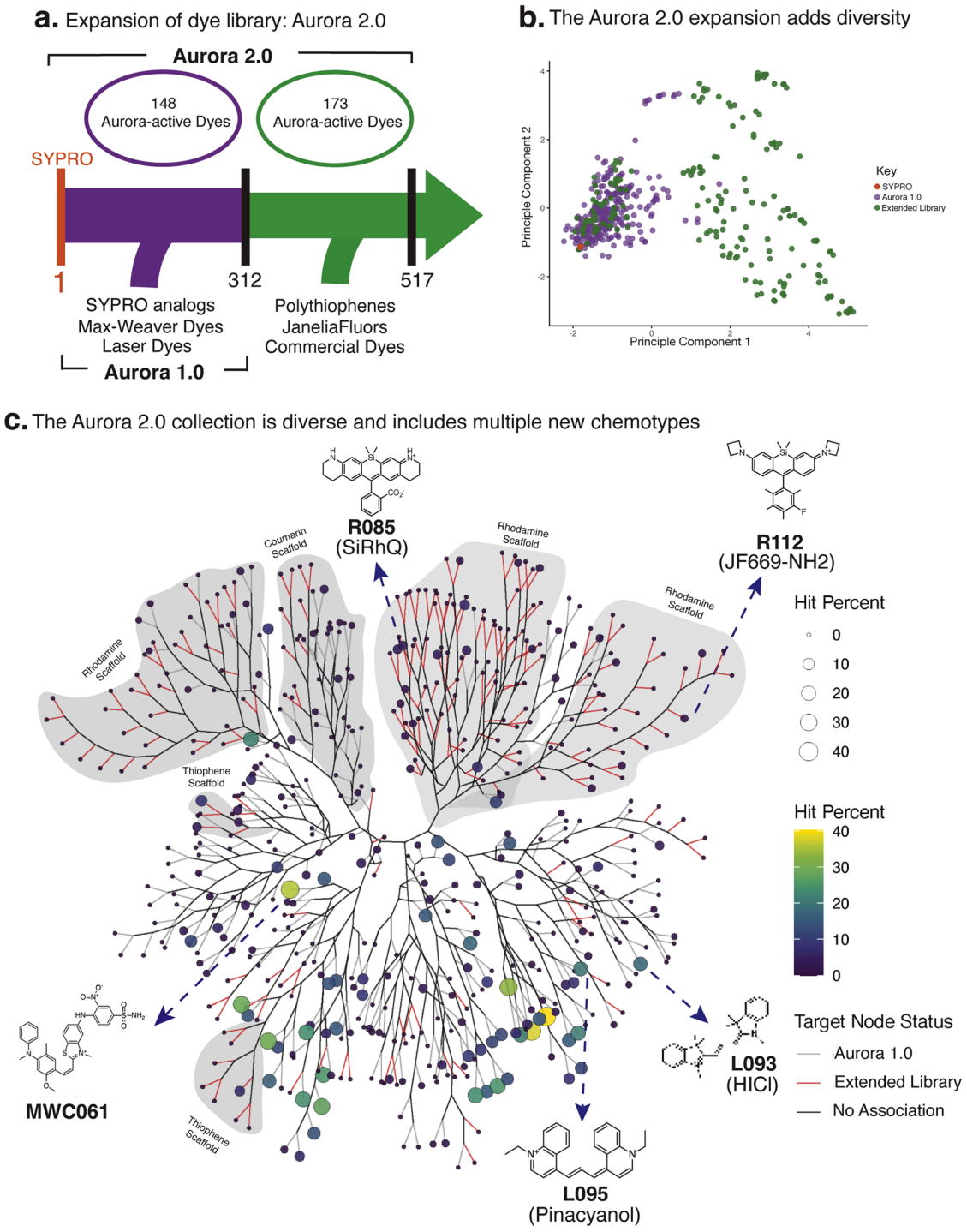

Fig. 2. Assembling a chemical diverse Aurora 2.0 dye collection. (a) The Aurora 1.0 library (purple) contains 312 dyes and 148 were found to interact with at least one protein. To expand on this collection, we added 205 dyes (green) from the JaneliaFluors, polythiophenes, and other commercial dyes. The Aurora 2.0 Library contains a total of 517 dyes, with 173 identified as interacting with at least one protein in paDSF experiments (see below). (b) A 1024-bit principal component analysis (PCA) was performed with Aurora 2.0, scaled by Aurora 1.0 (purple), the extended library (green), and SYPRO Orange (orange). PC1 represents the amount of variance based on the Morgan Fingerprints, and PC2 represents the second-most variance, such as changes in structure based on dye type. (c) A polar dendrogram determined using pairwise ECFP4 Tanimoto coefficient similarities followed by hierarchical clustering. Each circle represents an individual dye, and larger circles have a higher hit percentage against the protein test set (see below), Aurora 1.0 dyes are light grey branches, whereas the new extended library is labelled red. Additionally, highly related dye families are shadowed in grey and labelled by dye scaffold (rhodamine, thiophene). The chemical structures of some of the highest performing dyes are shown alongside their Aurora 2.0 number and/or common name.

3. Results

3.1. Building the Aurora 2.0 Library

To extend the capabilities of paDSF, we sought to add dyes to the Aurora 1.0 collection. Towards that objective, we curated the literature with a focus on adding chemotypes that are under-represented or not included in Aurora 1.0, ultimately selecting JaneliaFluors, Biotracker dyes and a set of diverse commercial molecules (Fig. 2**a**) [20,22–26]. The JaneliaFluor sub-collection consists of 144 dyes grouped into 15 distinct rhodamine-based scaffolds (**Supplemental Fig. 1**). The Biotracker dyes are polythiophenes that vary in length and spectral properties, which have been widely used in the imaging of amyloids. To quantify how these additions might expand the collection's chemical diversity, we determined 1024-bit Morgan fingerprints for each dye and then performed principal component analysis (PCA). This approach confirmed that the new additions increased the sampling of chemical space (Fig. 2**b**), where the first two principal components accounted for 14.9 % of the total variance (PC1: 9.9 %, PC2: 5.0 %). To illustrate this increased chemical diversity in a separate way, we calculated pairwise Tanimoto similarity coefficients and plotted the values on a dendrogram. In this representation, most of the new additions (Fig. 2**c**; red lines), such as the JaneliaFluor rhodamines and Biotracker polythiophenes, clustered separately from the other chemotypes, such as polymethines and merocyanines, which were already well-represented in Aurora 1.0 (Fig. 2**c**; grey lines). In addition, the new dyes extended parts of the existing collection; for example, the new coumarins added to the local diversity amongst that chemotype. While the overall chemical diversity is increased, the calculated clogP values of the Aurora 1.0 and new dyes are similar (**Supplemental Data 1**). Together, we conclude that, although Aurora 1.0 was already selected for chemical diversity, the extension to Aurora 2.0 further accentuated this property.

3.2. The Aurora 2.0 Library Further Extends the Scope of paDSF

Next, we collected a test panel of proteins for screening. We started with a subset (~65) of those proteins that had previously been screened against Aurora 1.0 [19]. These proteins had been chosen to vary in size and other structural features, such as helical content, percent disorder and hydrophobicity. Using this collection, it had previously been noted that smaller proteins tended to be harder targets [19]; therefore, we selected 43 additional proteins to add to the test set which were enriched in low molecular weight (< 30 kDa; **Supplemental Data 2**). These additional proteins also varied in the other key characteristics, such as percent disorder (**Supplementary Fig. 2**). It should be noted that this panel excludes membrane proteins, because of the expected complexity introduced by needing to include detergents or lipids. To illustrate the structural diversity of the test panel, we created AlphaFold3 models (**Supplementary Fig. 3**) [28], graphically showing the range of protein topologies and features. Together, we consider the resulting panel of ~100 proteins to be a representative set that could be used to rigorously explore the performance of the paDSF dyes.

We then screened the test proteins against the 517 compounds of the Aurora 2.0 collection to identify compatible protein-dye pairs. In these

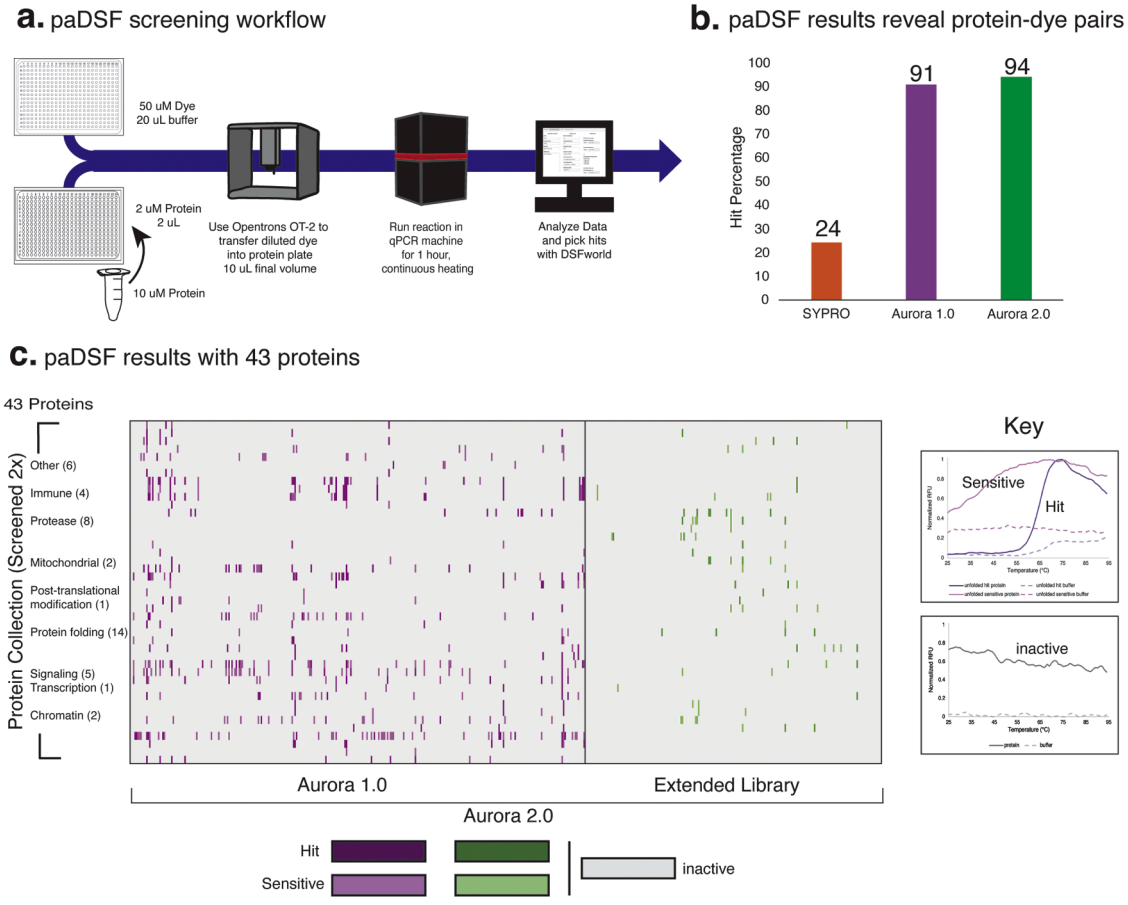

Fig. 3. Screens of the Aurora 2.0 collection produces dye-protein pairs for nearly all targets. (a) Schematic of the dye screening workflow, in which proteins and dyes are mixed and fluorescence measured as a function of temperature in an rtPCR instrument. Hits were selected using DSFWorld. (b) Sypro Orange was found to produce a meaningful T_{ma} value for 24 % of the target proteins, while Aurora 1.0 was successful for 91 % and Aurora 2.0 for 94 %. (c) Overview of the screening results, plotted as the dye similarity (top) against the protein test panel (side). Actives are indicated by a darker mark, sensitive dyes are shown in a lighter color and inactives are blank. Examples of a dye hit, a sensitive dye, and an inactive are shown in the key.

experiments, we used automated liquid handling to mix each protein (~10 μM) with each dye (~50 μM) in 384-well plates and then performed paDSF experiments in an rtPCR instrument (Fig. 3**a**). In the screens, we collected data at 6 excitation/emission pairs to allow for changes in either dye fluorescence intensity or wavelength, such that the workflow produced > 250,000 individual paDSF experiments and > 35 billion total datapoints. The resulting data was analyzed as previously described [19] and the initial actives were defined manually as "hits" (those dye-protein pairs that yielded clear T_{ma} values), "sensitive" (those dye-pairs that gave a signal, but with complex curve shapes) and "inactives" (those dye-protein pairs that did not yield a meaningful signal in any channel/temperature). Next, the "hit" and "sensitive" pairs were re-tested in validation experiments, in which the dye concentration was varied (see Methods; **Supplemental Data 3**). After removing false positives, the curves from the resulting "hits" were fit in DSFworld to calculate T_{ma} values. Together, we found that the Aurora 2.0 collection had a total of 173 dyes (33 %) that were paired with at least one protein. Moreover, the results clearly showed how paDSF experiments are improved by screening for optimized protein-dye pairs. For example, Sypro Orange was only able to identify T_{ma} values for 24 % of the targets, consistent with previous observations [19]. The original Aurora 1.0 collection performed significantly better, yielding useful dyes for 91 % of the targets. This overall hit rate is slightly lower than the previously reported one [19], likely because the new 43 test proteins were purposefully selected to be enriched for challenging targets. Finally, expansion of the dye collection to Aurora 2.0 improved the hit rate to 94 % (Fig. 3**b**).

To visually examine the global trends in the matches between dyes and proteins, the dyes were clustered by Tanimoto similarity and plotted as a function of the protein panel, grouped by approximate function (Fig. 3**c**). Here, we only focus on the results from the 43 new additions to the protein panel, but similar trends were seen in the larger set. From this analysis, a few observations are clear: (i) no dye works for every protein and (ii) each protein tends to work with multiple dyes from different chemotypes. Further, some chemotypes (such as the polymethines) seem slightly enriched in "hits", while others (such as coumarins) tend to produce fewer overall "hits" (also see Fig. 2**c**). However, no clear or obvious trends were seen in whether a dye would work for a specific protein in paDSF (see below); for example, even closely related dyes sometimes produced "hits" and "inactives" for the same protein target. This conclusion was further confirmed using Random Forest Classification, where active dyes failed to be recognized (specificity = 17.8 %, error = 82.2 %), emphasizing how a dye's structure alone cannot predict its paDSF activity. These findings support and extend the conclusions from previous work [19], highlighting the fact that pre-screening of a protein target against a diverse collection of dyes is currently the best approach to identify suitable pairs for paDSF experiments.

To understand if the paDSF experiments were returning meaningful results, we compared the calculated T_{ma} values of Sypro Orange-compatible proteins to the T_{ma} values calculated with the Aurora 2.0 library dyes using DSFWorld [4]. A Pearson's Correlation Test on the resulting data revealed a strong positive correlation between these values (Correlation = 0.83, $p = 0.021$, (**Supplemental Fig. 4a**). Similarly, we curated reported T_{ma} values from the literature, largely those collected from circular dichroism or DSF experiments, and compared them to the values from Aurora 2.0 dye experiments, showing that they are moderately correlated (Correlation = 0.74, $p = 3 \times 10^{-4}$, (**Supplemental Fig. 4b**). This correlation seems reasonable because the experimental conditions between these measurements (*i.e.,* buffer, concentration) are not always perfectly matched. Together, this data suggests that paDSF experiments produce accurate T_{ma} values, consistent with previous conclusions [19].

3.3. *Extension of the dye library improves the scope of targets*

With this data in-hand, we examined whether the new dyes in Aurora 2.0 indeed made a significant difference in the performance of paDSF. First, dyes in the Aurora 1.0 subcollection had 3-fold higher odds of being active (Fisher's exact test, $p = 5.72 \times 10^{-7}$, 95 % CI: 2.07–Inf). This conclusion is not surprising because the Aurora 1.0 dyes were initially curated from the literature as being environmentally sensitive and likely to bind proteins. However, among dyes that were active, no significant difference was observed in the number of proteins that were good pairs, termed the magnitude of the hit percentage (Wilcoxon rank-sum test, $p = 1.0$). Thus, both Aurora 1.0 and the extended library could produce high quality dye reagents, with the original collection being a more frequent contributor. This conclusion is perhaps best illustrated by plotting the hit percentage as a function of the two sub-collections (Fig. 4**a**), where the most frequently active dyes seem to be derived from the Aurora 1.0 collection, but the extended library also contributes important reagents. For example, we found that dyes in the Aurora 2.0 extension yielded matches for three difficult proteins: DnaJB8, trypsin inhibitor, and myosin heavy chain. More broadly, plotting the dyes that

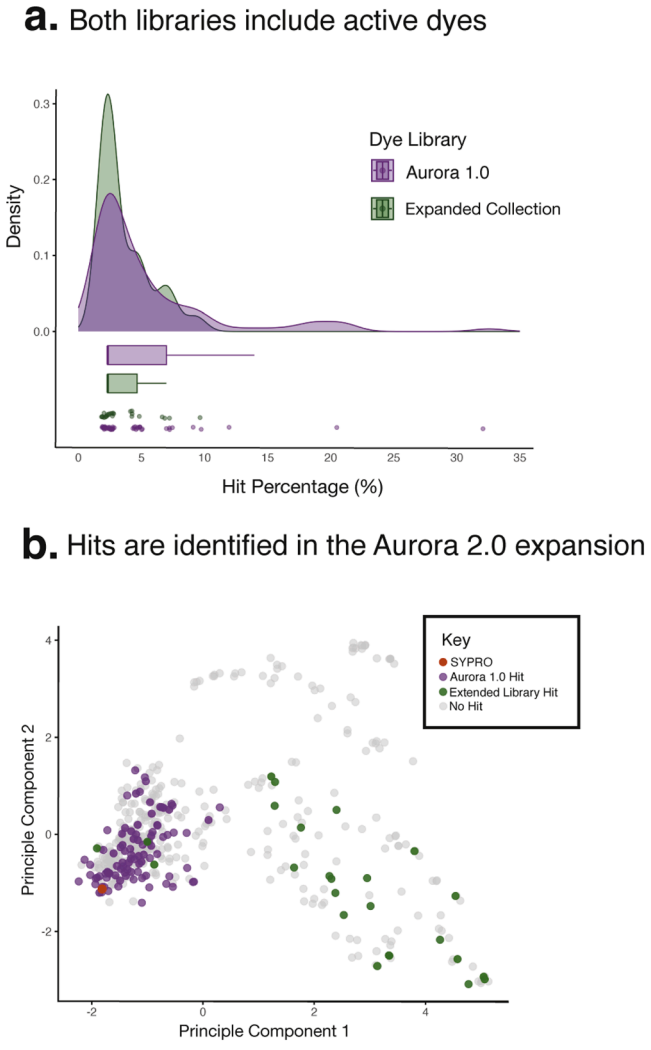

Fig. 4. The Aurora 2.0 collection further extends the scope of paDSF. (a) The success rates of Aurora 1.0 (purple) and the extended library (green) are shown. Hit percentage is defined for each dye as the percentage of the total proteins that it paired with. Results are shown as a density plot, box and whisker plot, and jittered plot. (b) The PCA plot (see Fig. 2a) re-colored to indicate "hit" dyes from Aurora 1.0 (purple) or the extended library (green). Also shown are Sypro Orange (orange) and inactive dyes (grey).

produced at least one "hit" onto the PCA projections confirmed that the increased chemical space was important in expanding the scope of paDSF (Fig. 4**b**; green spots). Thus, we conclude that Aurora 2.0 improves the overall hit rate (94 %) and produces active dyes for previously inaccessible targets.

3.4. The Features that Determine a Good Dye-Protein Pair are Complex

What features of a dye or protein predict whether they will be a good match? One might imagine that chemical features of the protein would predict a match and that the large amount of data collected here might reveal those trends. To test this idea, we analyzed multiple parameters of the target proteins [29], such as percent disorder, helical content, hydrophobicity, solvent accessible surface areas (SASA), and molecular weight, but found no clear trends that would predict the identified dyes (**Supplemental Fig. 5**). Likewise, we found that some dyes worked well for structurally disparate proteins, while others did not work well for even closely related protein family members (see below). Thus, there does not appear to be any immediately recognizable feature(s) of a protein or a dye that simply predicts whether they will form a good pair. Fortunately, a dye screens can be accomplished rapidly (~2 hrs / protein), so an empirical approach to the discovery of optimal paDSF dye(s) for a specific target or application seems acceptable from the perspective of time and cost.

3.5. Focused protein set confirms the complexity of predicting dye-protein pairs

To further explore the question of whether dyes might have a preference for proteins with similar sequences, we purified a series of highly related proteins from the J-domain protein (JDP) family [30,31]. Briefly, the JDPs act as molecular chaperones and they all contain a highly conserved J-domain, in addition to other, variable domains, such as Zinc-finger (ZFs) regions, C-terminal domain (CTDs) and tetratricopeptide repeat (TPR) motifs (Fig. 5**a**). Thus, we hypothesized that, if dyes are recognizing shared features of a protein, then we might find dyes that would work for all members of this focused set of targets (or at least the most closely related ones). To ask this question, we screened the JDPs against the Aurora 2.0 collection, revealing a total of 29 "hits". We found that only four of the dyes interacted with three or more proteins in the family (Fig. 5**b**, red lines). Moreover, the chemical structures of these four dyes are dissimilar, suggesting that scaffold similarity does not drive protein preferences. For example, we found that dye C001 performed relatively well, allowing accurate T_{ma} value measurements

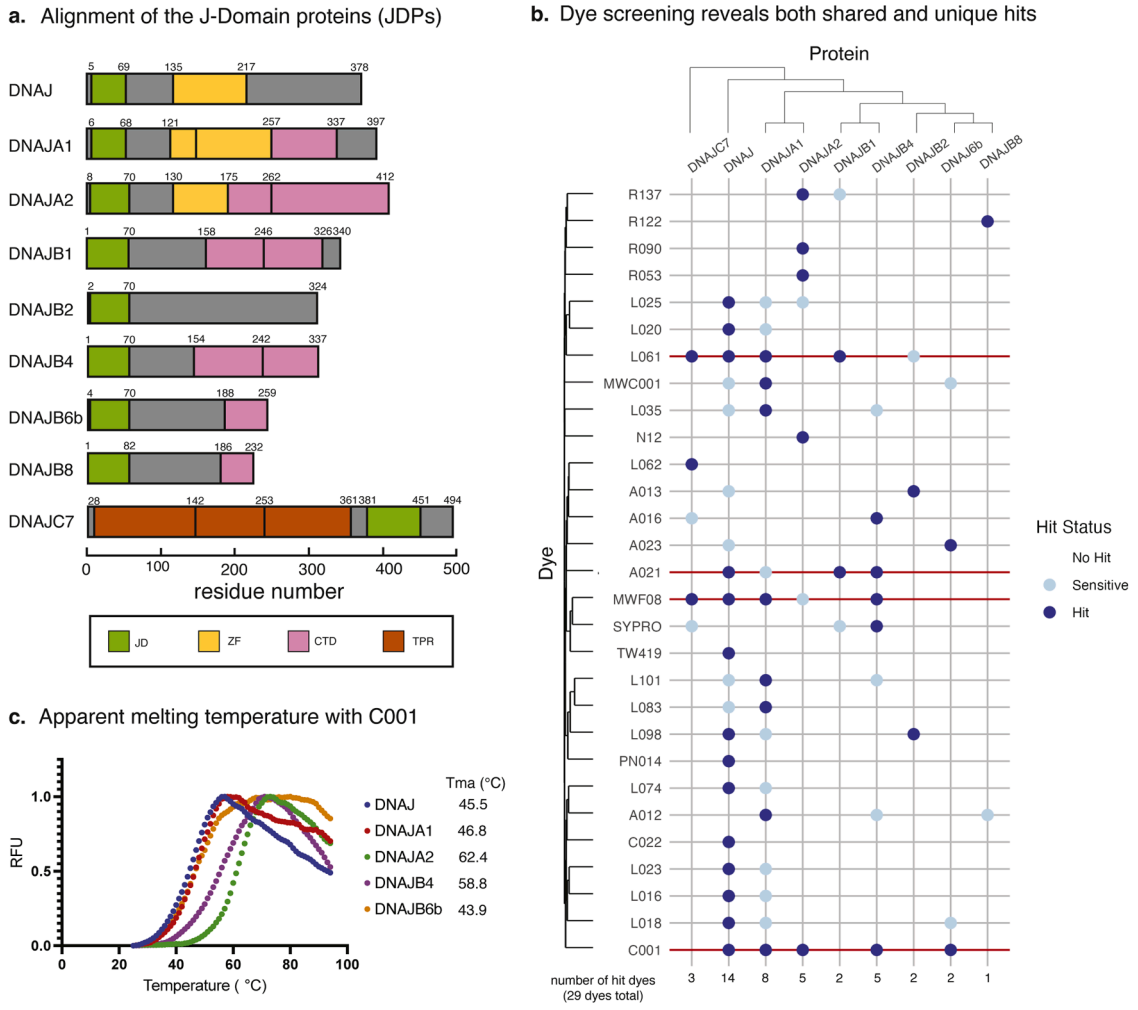

Fig. 5. A focused screen of similar proteins supports the complexity of predicting dye-protein pairs. (a) Domain architecture of the JDPs, highlighting their similarities and differences. The founding member of the family, DNAJ, from *E. coli* is shown alongside a subset of the human JDPs. Domains are labelled: J-domain (green), zinc finger (yellow), C-terminal domains (CTDs; pink), and TPR domains (orange). (b) Comparison of paDSF activity, with the y-axis a dendogram of dye similarity, and the x-axis a dendrogram of protein similarity. Dye-protein pairs are shown as blue, a sensitive dye is marked as light blue, and inactives are blank. Dyes that work for three or more proteins are highlighted with a red line. (c) Representative, normalized paDSF curves for a subset of the JDPs, using the dye C001. Results show a single experiment that is representative of those performed in independent triplicates.

for half of the proteins: DnaJ, DnaJA1, DnaJA2, DnaJB4 and DnaJB8b (Fig. 5**c**), but that this same dye did not work well for the closely related DnaJB1 (which is 73.9 % identical and 92.8 % similar to DnaJB4). Together, these results support the idea that specific protein-dye pairs cannot, at this stage, readily be determined by sequence similarity or dye structure alone.

3.6. Aurora 2.0 also contains fluoroprobes that bind the native, folded state

Recent work by Carroll et al. extended the use of the Aurora 1.0 library beyond paDSF applications [40]. Specifically, they combined the Aurora 1.0 collection with a series of structurally distinct amyloid fibril polymorphs and asked whether any of the dyes might exhibit increased fluorescence for only a subset of the samples [40]. This alternative use of the Aurora dyes is quite different from paDSF, as the "hits" must be able to bind to the folded protein, rather than to the thermally unfolded state (s).

We wondered whether Aurora 2.0 might also include dyes that would bind to the folded state of proteins. To search for such dyes, we re-analyzed the screen of the 43 test proteins to look for pairs in which the initial fluorescence is high. These pairs would have been rejected as "inactives" in our initial triage scheme for paDSF experiments, but here we wanted to specifically note them. In this selection, we also favored dye-protein pairs in which the fluorescence intensity decreases during heating, as this behavior might indicate a loss of binding during unfolding (Fig. 6**a**). Satisfying, this analysis revealed many dyes that seemed to interact with the folded, native states. Interestingly, the extended Aurora 2.0 library was found to be 2.08x more likely to produce a hit than Aurora 1.0 ($p = 0.00188$, OR = 0.47, 95 % CI: [0.00, 0.73]; Fisher's Exact Test), suggesting that some scaffolds are more likely to produce this behavior than others. This conclusion was further supported by mapping the "folded protein hits" onto the chemical similarity dendrogram (Fig. 6**b**), where a subset of the rhodamines from the expanded library was found to be enriched. Similarly, plotting the results by protein class and dye collection showed an enrichment for the extended library (Fig. 6**c**). We note that these studies include a control without protein to rule out temperature effects on dye fluorescence, such that the signal is most likely from direct binding to the target.

Similar to what we observed in the paDSF experiments, we could not identify clear patterns in the protein-dye pairs that would allow predictions of an interaction with the folded state. For example, using Random Forest Classifications, it was found that active dyes were inaccurately classified (specificity = 16.2 %, error = 83.8 %), resulting in an OOB error rate of 15.7 %. Thus, it seems difficult to predict whether a dye will interact with the folded state based on its chemical structure alone. Consistent with this conclusion, we found that there is only a moderate Pearson's correlation between protein disorder and whether a dye will interact with a protein (Correlation = −0.48, $p = 0.001$), and no other protein feature was found to correlate (**Supplementary Fig. 6**). To explain this modest correlation, we speculate that disordered proteins may be less likely to provide stable sites for the dye. Despite the lack of clear predictive features, these results support the use of Aurora 2.0 dyes as fluoroprobes for the detection of folded proteins.

4. Discussion

DSF has proven to be a useful platform for experiments such as measuring protein stability and estimating ligand binding, but its use has traditionally been limited to those proteins that are compatible with Sypro Orange. To expand the scope of this technology, we introduce Aurora 2.0, an expanded dye collection for use in paDSF. Using this collection, dyes were identified for 94 % of proteins in our test set of >100 diverse proteins. In comparison, Sypro Orange worked for < 30 % of proteins (see Fig. 3**b**). With some exceptions, the molecules in Aurora 2.0 are commercially available (see **Supplemental Data 1**) or synthesized in a few steps, such that paDSF workflows using this dye prescreening approach should be accessible in many settings.

One use of paDSF is to identify chemical inhibitors and it has been reported that having multiple dyes for each protein target is a benefit during this type of workflow. For example, when a ligand or inhibitor is found to be incompatible with one dye (*e.g.,* insolubility, spectral overlap, shared binding site with a ligand, *etc.*), that dye can be swapped out for another chemotype [32]. Thus, one benefit of the expanded Aurora 2.0 collection is that it is also likely to provide useful secondary dyes, even for proteins that already have a good pair in the Aurora 1.0 collection.

In these studies, we hoped to uncover the features that dictate protein-dye pairs, such that we might predict whether a specific protein would be a good target for paDSF. However, when we attempted to correlate hit rate with protein features, such as molecular mass, hydrophobicity, helical content or percent disorder, we failed to identify any meaningful trends (see **Supplementary Fig. 5**). Thus, it remains challenging to predict whether a protein will be a good target, or *de novo* match a dye to a given protein. Rather, we posit that an empirical approach might be the best course of action at present. This conclusion is illustrated by our focused screen of the JDPs, which despite their close sequence relationships, were found to work with a diverse set of dyes (see Fig. 5**b**). We speculate that the challenge in predicting dye-protein pairs might arise from the fact that the dye interaction occurs within a globular, unfolded state of the protein, which is poorly characterized or modelled.

Finally, we speculate that the dyes of Aurora 2.0 could potentially be used for purposes outside of paDSF. Here, we note that a subset of dyes binds to the folded, native state of proteins (see Fig. 6**c**), such that they might be used as fluoroprobes to detect these targets. Such "turn-on" dyes may be useful in contexts such as imaging or histopathology, where precise labeling is desired. Indeed, many research groups are pursuing fluorescent molecules that can be used to track protein position and/or conformation [33–39]. We reason that the physicochemical properties that drive dye activity in paDSF could be leveraged towards these types of applications, such that Aurora 2.0 could be a rich source of potential fluoroprobes.

CRediT authorship contribution statement

Annemarie F. Charvat: Writing – review & editing, Writing – original draft, Visualization, Investigation, Formal analysis, Data curation. **Kayleigh Mason-Chalmers:** Writing – review & editing, Writing – original draft, Visualization, Investigation, Formal analysis, Data curation. **Aneta Grabinska-Rogala:** Investigation. **Shloka Shivakumar:** Investigation. **Zachary Gale-Day:** Writing – review & editing, Visualization, Supervision. **Taiasean Wu:** Writing – review & editing, Supervision, Software, Conceptualization. **Zoe Millbern:** Resources, Investigation. **Jonathan B. Grimm:** Resources. **Emma C. Carroll:** Supervision, Investigation. **K. Peter R. Nilsson:** Writing – review & editing, Resources. **Luke D. Lavis:** Writing – review & editing, Resources. **Nelson R. Vinueza:** Writing – review & editing, Supervision, Resources, Project administration, Funding acquisition. **Jason E. Gestwicki:** Writing – review & editing, Writing – original draft, Supervision, Project administration, Funding acquisition, Conceptualization.

Declaration of interest

The authors declare the following financial interests/personal relationships which may be considered as potential competing interests:

Jason E. Gestwicki reports financial support was provided by National Institutes of Health. Emma Carroll reports financial support was provided by National Institutes of Health. Nelson Vinueza reports financial support was provided by National Institutes of Health. Patents and patent applications covering azetidine- and deuterium-containing dyes (with inventors J.B.G. and L.D.L.) are assigned to HHMI. If there

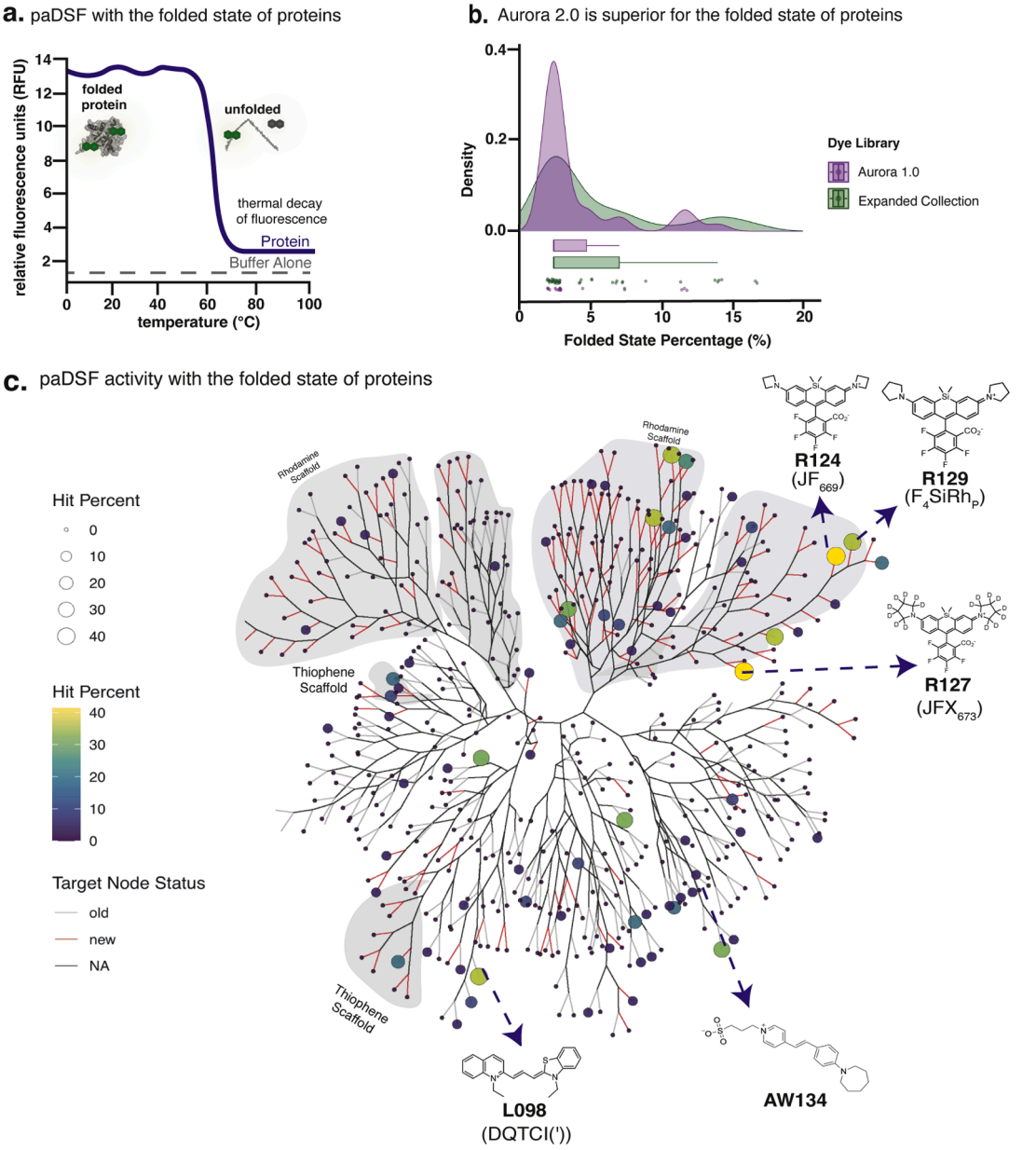

(caption on next page)

Fig. 6. The Aurora 2.0 collection can be used to identify fluoroprobes that bind to the folded, native state. (a) Illustration of the expected behavior of a "hit" that binds the folded state. The dye-protein pair has high initial fluorescence, which decreases as the protein thermally unfolds. (b) The distribution of the "hits" that bind to the folded state (*e.g.*, have high initial fluorescence) for each dye separated by library: Aurora 1.0 (purple) and extended library (green), shown by a density plot, a box and whisker plot, and a jittered plot. (c) The chemical similarity tree (from Fig. 3) re-labelled to indicate the percentage of proteins bound by each dye in the folded state. The chemical structures of some of the best performing dyes are shown. (d) A heat map of the results, separated by Aurora 1 (purple) and the expanded library (green). Representative DSF curves are shown for a "hit", an "inactive" and a "sensitive".

are other authors, they declare that they have no known competing financial interests or personal relationships that could have appeared to influence the work reported in this paper.

Lead contact

Further information and requests for resources should be directed to and will be fulfilled by the lead contact Jason Gestwicki

Data availability statement

All raw data, including dye screening, plus algorithms and software used in this work is available at (10.5281/zenodo.15792912). The software for dye screening and analysis is available at: https://ucsfdyescreens.shinyapps.io/screen_analysis and DSFWorld is available at: https://gestwickilab.shinyapps.io/dsfworld. The description of the dye collection is listed in **Supplementary Data 1**, the protein test panel is available in **Supplementary Data 2** and the validation screening results are in **Supplementary Data 3**.

Statements and declarations

This work was funded by Howard Hughes Medical Institute (to L.D. L.) and the NIH, including grants R01GM141299 (N.R.V. and J.E.G.), T32GM145460 (J.E.G.), F31AR081704 (to Z.G.-D.) and F32AG076281 (E.C.C.). Additional support was provided by NSF Graduate Research Fellowship 1000259744 (to T.W.).

Acknowledgements

The authors thank the following individuals for providing proteins for the test panel: Anthony Yung, Shweta Devi, Saugat Pokhrel, Wyatt Powell, Katie Holland, Alex Long, Ben Ahn, Oleta Johnson, Jennifer Rauch, Caiquin Wang, Chad Altobelli, Lapon Visitvorant, Steve Olson, Hannah Addis, Erin Carlson, Lena Bergmann, Brian Zhou, Jules Brunello, James Fraser, John Chorba, Nicole Lynn Inniss, Karla Satchell, Judd Hultquist, Kelly Bachta, Ryan Kich, Seth Rubin, Carina Villegas, Phuong Nguyen, Pamela England, Isabelle Taylor, Maggie O'Hara, and Matthew Callahan. We also thank Nathaniel Sin, Craig Muir, Ian Muir, Madeline Lequang, Jez Lafuente Revalde, Michelle Arkin, Jeffrey Nietz, Sarah McCormack, Matthew Sigman and Pranathi Kande for providing advice and experimental assistance.

Supplementary materials

Supplementary material associated with this article can be found, in the online version, at doi:10.1016/j.slasd.2025.100259.

References

[1] Gao K, Oerlemans R, Groves MR. Theory and applications of differential scanning fluorimetry in early-stage drug discovery. Biophys Rev 2020;12:85–104.
[2] Simeonov A. Recent developments in the use of differential scanning fluorometry in protein and small molecule discovery and characterization. Expert Opin Drug Discov 2013;8:1071–82.
[3] Niesen FH, Berglund H, Vedadi M. The use of differential scanning fluorimetry to detect ligand interactions that promote protein stability. Nat Protoc 2007;2:2212–21.
[4] Wu T, Gale-Day ZJ, Gestwicki JE. DSFworld: a flexible and precise tool to analyze differential scanning fluorimetry data. Protein Sci 2024;33:e5022.
[5] Martin-Malpartida P, Hausvik E, Underhaug J, Torner C, Martinez A, Macias MJ. HTSDSF Explorer, A novel tool to analyze high-throughput DSF screenings. J Mol Biol 2022;434:167372.
[6] Fedorov O, Niesen FH, Knapp S. Kinase inhibitor selectivity profiling using differential scanning fluorimetry. Methods Mol Biol 2012;795:109–18.
[7] Sun NN, Xu QF, Yang MD, Li YN, Liu H, Tantai W, Shu GW, Li GL. A high-throughput differential scanning fluorimetry method for rapid detection of thermal stability and iron saturation in lactoferrin. Int J Biol Macromol 2024;267:131285.
[8] Malik K, Matejtschuk P, Thelwell C, Burns CJ. Differential scanning fluorimetry: rapid screening of formulations that promote the stability of reference preparations. J Pharm Biomed Anal 2013;77:163–6.
[9] Nie M, Liu Y, Huang X, Zhang Z, Zhao Q. Microtiter plate-based differential scanning fluorimetry: a high-throughput method for efficient formulation development. J Pharm Sci 2022;111:2397–403.
[10] Menzen T, Friess W. High-throughput melting-temperature analysis of a monoclonal antibody by differential scanning fluorimetry in the presence of surfactants. J Pharm Sci 2013;102:415–28.
[11] Khadiullina R, Mirgayazova R, Davletshin D, Khusainova E, Chasov V, Bulatov E. Assessment of thermal stability of mutant p53 proteins via differential scanning fluorimetry. Life 2022:13.
[12] Lea WA, Simeonov A. Differential scanning fluorometry signatures as indicators of enzyme inhibitor mode of action: case study of glutathione S-transferase. PLoS One 2012;7:e36219.
[13] Wu T, Hornsby M, Zhu L, Yu JC, Shokat KM, Gestwicki JE. Protocol for performing and optimizing differential scanning fluorimetry experiments. STAR Protoc 2023;4:102688.
[14] DeSantis K, Reed A, Rahhal R, Reinking J. Use of differential scanning fluorimetry as a high-throughput assay to identify nuclear receptor ligands. Nucl Recept Signal 2012;10:e002.
[15] Hansel CS, Lanne A, Rowlands H, Shaw J, Collier MJ, Plant H. High-throughput differential scanning fluorimetry (DSF) and cellular thermal shift assays (CETSA): shifting from manual to automated screening. SLAS Technol 2023;28:411–5.
[16] Makley LN, McMenimen KA, DeVree BT, Goldman JW, McGlasson BN, Rajagopal P, Dunyak BM, McQuade TJ, Thompson AD, Sunahara R, Klevit RE, Andley UP, Gestwicki JE. Pharmacological chaperone for alpha-crystallin partially restores transparency in cataract models. Science 2015;350:674–7.
[17] Hellman LM, Yin L, Wang Y, Blevins SJ, Riley TP, Belden OS, Spear TT, Nishimura MI, Stern LJ, Baker BM. Differential scanning fluorimetry based assessments of the thermal and kinetic stability of peptide-MHC complexes. J Immunol Methods 2016;432:95–101.
[18] McClure RA, Williams JD. Impact of mass spectrometry-based technologies and strategies on chemoproteomics as a tool for drug discovery. ACS Med Chem Lett 2018;9:785–91.
[19] Wu T, Yu JC, Suresh A, Gale-Day ZJ, Alteen MG, Woo AS, Millbern Z, Johnson OT, Carroll EC, Partch CL, Fourches D, Vinueza NR, Vocadlo DJ, Gestwicki JE. Protein-adaptive differential scanning fluorimetry using conformationally responsive dyes. Nat Biotechnol 2025;43:106–13.
[20] Kuenemann MA, Szymczyk M, Chen Y, Sultana N, Hinks D, Freeman HS, Williams AJ, Fourches D, Vinueza NR. Weaver's historic accessible collection of synthetic dyes: a cheminformatics analysis. Chem Sci 2017;8:4334–9.
[21] Devi S, Charvat A, Millbern Z, Vinueza N, Gestwicki JE. Exploration of the binding determinants of protein phosphatase 5 (PP5) reveals a chaperone-independent activation mechanism. J Biol Chem 2024;300:107435.
[22] Grimm JB, Tkachuk AN, Xie L, Choi H, Mohar B, Falco N, Schaefer K, Patel R, Zheng Q, Liu Z, Lippincott-Schwartz J, Brown TA, Lavis LD. A general method to optimize and functionalize red-shifted rhodamine dyes. Nat Methods 2020;17:815–21.
[23] Klingstedt T, Aslund A, Simon RA, Johansson LB, Mason JJ, Nystrom S, Hammarstrom P, Nilsson KP. Synthesis of a library of oligothiophenes and their utilization as fluorescent ligands for spectral assignment of protein aggregates. Org Biomol Chem 2011;9:8356–70.
[24] Grimm JB, Klein T, Kopek BG, Shtengel G, Hess HF, Sauer M, Lavis LD. Synthesis of a far-red photoactivatable silicon-containing rhodamine for super-resolution microscopy. Angew Chem Int Engl 2016;55:1723–7.
[25] Shirani H, Appelqvist H, Back M, Klingstedt T, Cairns NJ, Nilsson KPR. Synthesis of thiophene-based optical ligands that selectively detect tau pathology in Alzheimer's disease. Chemistry 2017;23:17127–35.
[26] Klingstedt T, Shirani H, Ghetti B, Vidal R, KP RN. Thiophene-based optical ligands that selectively detect abeta pathology in Alzheimer's disease. Chembiochem 2021;22:2568–81.
[27] Mitternacht S. FreeSASA: an open source C library for solvent accessible surface area calculations. F1000Res 2016;5:189.
[28] Abramson J, Adler J, Dunger J, Evans R, Green T, Pritzel A, Ronneberger O, Willmore L, Ballard AJ, Bambrick J, Bodenstein SW, Evans DA, Hung CC, O'Neill M, Reiman D, Tunyasuvunakool K, Wu Z, Zemgulyte A, Arvaniti E, Beattie C, Bertolli O, Bridgland A, Cherepanov A, Congreve M, Cowen-Rivers AI, Cowie A, Figurnov M, Fuchs FB, Gladman H, Jain R, Khan YA, Low CMR, Perlin K,

Potapenko A, Savy P, Singh S, Stecula A, Thillaisundaram A, Tong C, Yakneen S, Zhong ED, Zielinski M, Zidek A, Bapst V, Kohli P, Jaderberg M, Hassabis D, Jumper JM. Accurate structure prediction of biomolecular interactions with AlphaFold 3. Nature 2024;630:493–500.

[29] Lotthammer JM, Ginell GM, Griffith D, Emenecker RJ, Holehouse AS. Direct prediction of intrinsically disordered protein conformational properties from sequence. Nat Methods 2024;21:465–76.

[30] Ryder BD, Wydorski PM, Hou Z, Joachimiak LA. Chaperoning shape-shifting tau in disease. Trends Biochem Sci 2022;47:301–13.

[31] Kampinga HH, Craig EA. The HSP70 chaperone machinery: j proteins as drivers of functional specificity. Nat Rev Mol Cell Biol 2010;11:579–92.

[32] Schuller M, Correy GJ, Gahbauer S, Fearon D, Wu T, Diaz RE, Young ID, Carvalho Martins L, Smith DH, Schulze-Gahmen U, Owens TW, Deshpande I, Merz GE, Thwin AC, Biel JT, Peters JK, Moritz M, Herrera N, Kratochvil HT, Consortium QSB, Aimon A, Bennett JM, Brandao Neto J, Cohen AE, Dias A, Douangamath A, Dunnett L, Fedorov O, Ferla MP, Fuchs MR, Gorrie-Stone TJ, Holton JM, Johnson MG, Krojer T, Meigs G, Powell AJ, Rack JGM, Rangel VL, Russi S, Skyner RE, Smith CA, Soares AS, Wierman JL, Zhu K, O'Brien P, Jura N, Ashworth A, Irwin JJ, Thompson MC, Gestwicki JE, von Delft F, Shoichet BK, Fraser JS, Ahel I. Fragment binding to the Nsp3 macrodomain of SARS-CoV-2 identified through crystallographic screening and computational docking. Sci Adv 2021:7.

[33] You S, Nguyen T, Li-Ma C, Bollong MJ. Identification of tunable, environmentally responsive fluorogenic dyes by high-throughput screening. ACS Chem Biol 2024; 19:2041–9.

[34] Munan S, Chang YT, Samanta A. Chronological development of functional fluorophores for bio-imaging. Chem Commun 2024;60:501–21.

[35] Spearman AL, Lin EY, Mobley EB, Chmyrov A, Arus BA, Turner DW, Garcia CA, Bui K, Rowlands C, Bruns OT, Sletten EM. High-resolution multicolor shortwave infrared dynamic In vivo imaging with chromenylium nonamethine dyes. J Am Chem Soc 2025;147:17384–93.

[36] Frei MS, Sanchez SA, He X, Liu L, Schneider F, Wang Z, Hakozaki H, Li Y, Lyons AC, Rohm TV, Olefsky JM, Shi L, Schoneberg J, Fraser SE, Mehta S, Wang Y, Zhang J. Far-red chemigenetic kinase biosensors enable multiplexed and super-resolved imaging of signaling networks. Nat Biotechnol 2025.

[37] Rudd AK, Mittal N, Lim EW, Metallo CM, Devaraj NK. A small molecule fluorogenic probe for the detection of sphingosine in living cells. J Am Chem Soc 2020;142: 17887–91.

[38] Seal S, Trapotsi MA, Spjuth O, Singh S, Carreras-Puigvert J, Greene N, Bender A, Carpenter AE. Cell Painting: a decade of discovery and innovation in cellular imaging. Nat Methods 2025;22:254–68.

[39] Ma J, Luo F, Hsiung CH, Dai J, Tan Z, Ye S, Ding L, Shen B, Zhang X. Chemical control of fluorescence lifetime towards multiplexing imaging. Angew Chem Int Engl 2024;63:e202403029.

[40] Carroll EC, Yang H, Jones JG, Oehler A, Charvat AF, Montgomery KM, Yung A, Millbern Z, Vinueza NR, Degrado WF, Mordes DA, Condello C, Gestwicki JE. Methods for high throughput discovery of fluoroprobes that recognize tau fibril polymorphs. BioRxiv 2024. https://doi.org/10.1101/2024.09.02.610853.